Analysis Methods for Electron Radiography Based on Laser-Plasma Accelerators

G. Bruhaug,[1,2] M. S. Freeman,[3] H. G. Rinderknecht,[1] L. P. Neukirch,[3] C. H. Wilde,[3] F. E Merrill,[3] J. R. Rygg,[1,2,4] M. S. Wei,[1] G. W. Collins,[1,2,4] and J. L. Shaw[1]

[1]Laboratory for Laser Energetics, University of Rochester
[2]Department of Mechanical Engineering, University of Rochester
[3]Los Alamos National Laboratory
[4]Department of Physics and Astronomy, University of Rochester

Electron radiography (eRad) is a proven, highly penetrative radiography technique that has typically been performed with traditional linear accelerators (LINAC's).[1,2] Recent work has extended electron radiography techniques into the laser-plasma acceleration (LPA) regime[3,4] with an emphasis on the radiography of laser-driven dynamics systems.

To compare LPA eRad to traditional LINAC eRad and other radiography methods, the resolution and transmission of said source must be determined. In addition, LPA-based eRad can modify the properties of the object being radiographed via a laser-generated plasma if the drive laser is not dumped.[4] Here we present analysis methods to determine the resolution for LPA eRad that include accounting for image distortion caused by the drive laser.

A polychromatic electron beam generated via LPA with an average energy of ~20 MeV and a bunch charge of up to 700 nC was used to radiograph various test objects in both contact and projection radiography.[4,5] All radiographs were taken using MS (multipurpose standard) image plates with 12.5 μm of aluminium in front to dump the laser. MeV-scale electrons have been found to have a relatively flat energy response in image plates and are detected at high efficiency.[6] All images were then analyzed via the software ImageJ[7] and the final scans were gray-scale balanced to make the clearest images.

It should be noted that the majority of the LPA drive laser is transmitted through the LPA plasma source. In the projected configuration the laser impacts the front face of the projection radiography object with ~10^{15} W/cm^2 intensity and ~20 to 100 J of laser energy depending on drive specifics. This excess laser energy will impact the target ~100 fs before the electron beam arrives and will generate plasma on the front surface of the object.[4] Consequently, even these supposedly "static" radiography objects were, in reality, laser-ablated dynamic radiography objects.

Contact radiography provided the ability to remove the transverse structure of the electron beam using the image plate placed in front of the radiography object to record the beam transverse structure before the beam passes through the radiography object. Transverse structure from the beam adds additional blurring to the radiograph that can be eliminated via image division using the software ImageJ.[7] Using these adjusted images, image resolution was determined by creating a box lineout tens of pixels wide across the edges generated by the thickness steps in the radiography object [see Fig. 1(a)] and across the edges of the holes in each thickness step. An error function of the form shown in Eq. (1) was then fitted to the lineout as shown in Fig. 1(b).

$$y = a + b\,\mathrm{erf}\left(\frac{x-c}{d}\right). \tag{1}$$

Variables *a*, *b*, *c*, and *d* are fitting parameters for the error function with *d* giving the resolution. This procedure was repeated across all edges of holes, all edges of the object, and all thickness steps on the object. The results were then averaged for each thickness of material to produce a final resolution at each thickness of material.

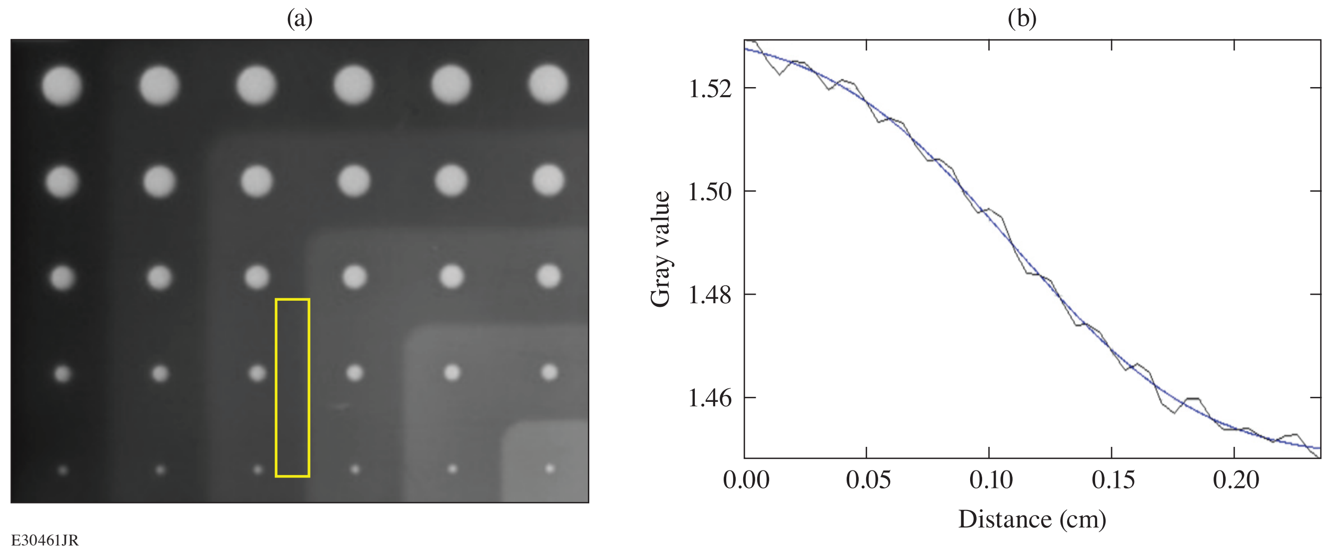

Figure 1
(a) Example of a resolution measurement across thickness step edge for tungsten contact radiography object. The yellow box across the thickness step edge shows the outline of the data used to make the measurement. (b) Lineout of boxed region from (a) (black curve) and error function fit (blue curve).

To determine the resolution in projection radiography, the final image plate scan is taken and gray scale is balanced for maximum clarity. Box lineouts tens of pixels wide are then taken across the central step in object thickness as well as the object outer edges and hole edges. An error function is fitted to the lineouts and the resolution taken from that function is shown in Fig. 2. These measurements are performed multiple times around the resolution measurement point of interest (i.e., an edge or a step-in material thickness) and then averaged to determine a final value.

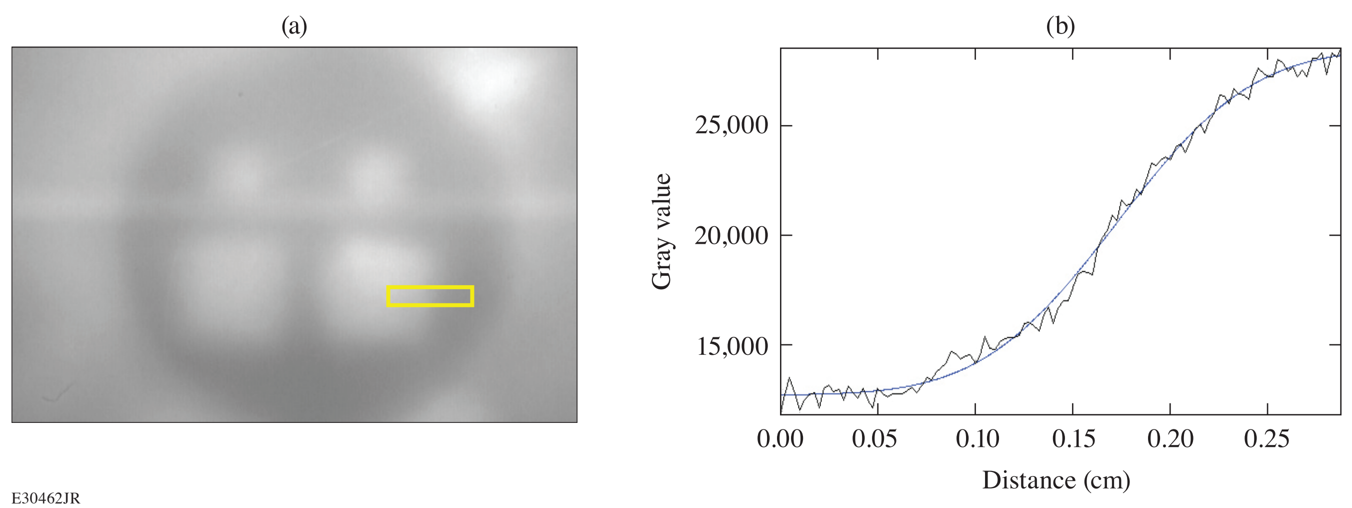

Figure 2
(a) Example of a resolution measurement across a hole for tungsten projection radiography object. The yellow box across the thickness step edge shows the outline of the data used to make the measurement. (b) Lineout of boxed region from (a) (black curve) and error function fit (blue curve).

Plasma-generated electric fields in laser-ablated targets can be roughly measured by measuring the size of features in the eRad image and estimating the field strength needed to produce those features. When measuring the sizes of the static projection radiography objects, it was noticed that the resulting radiographs were ~1.5× smaller than expected, as illustrated in Fig. 3. Previous data suggest that this size discrepancy was caused by plasma-generated electric fields acting like an electrostatic lens on the electron beam.[8] Using the average electron beam energy of ~20 MeV (Ref. 5), it was determined that the electric field that corresponded to ~1 GV/m (Ref. 4) would generate the magnification discrepancies seen. This is well in line with previous laser-plasma electric-field strengths at this laser intensity.[8]

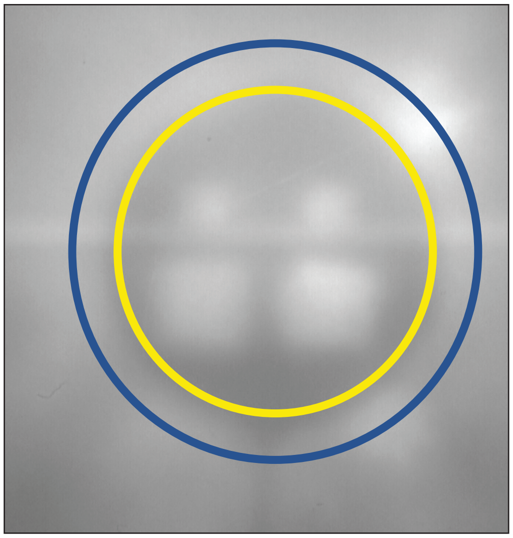

E30463JR

Figure 3
Projected radiograph of tungsten radiography object showing the size discrepancy caused by the plasma electric field focusing of the electron beam. The blue outline shows the expected image size of ~1.8 cm if there was no plasma focusing, and the yellow circle shows the measured diameter of ~1.2 cm.

This material is based upon work supported by the Department of Energy National Nuclear Security Administration under Award Number DE-NA0003856, the U.S. Department of Energy under Awards DE-SC00215057, the University of Rochester, and the New York State Energy Research and Development Authority.

1. F. Merrill *et al.*, Nucl. Instrum. Methods Phys. Res. B **261**, 382 (2007).
2. F. E. Merrill *et al.*, Appl. Phys. Lett. **112**, 144103 (2018).
3. W. Schumaker *et al.*, Phys. Rev. Lett. **110**, 015003 (2013).
4. G. Bruhaug *et al.*, Sci. Rep. **13**, 2227 (2023).
5. J. L. Shaw *et al.*, Sci. Rep. **11**, 7498 (2021).
6. G. Boutoux *et al.*, Rev. Sci. Instrum. **86**, 113304 (2015).
7. C. A. Schneider, W. S. Rasband, and K.W. Eliceiri, Nat. Methods **9**, 671 (2012).
8. J. L. Dubois *et al.*, Phys. Rev. E **89**, 013102 (2014).